

Structure of spin polarons in the t - t' - t'' - J^z model

J. Bala^a

Institute of Physics, Jagellonian University, Reymonta 4, 30059 Kraków, Poland

Received 11 January 2000

Abstract. We calculate the Green function in the t - t' - t'' - J^z model and analyze the deformation of the quantum Néel state in the presence of a moving hole. Solving the problem in a self-consistent Born approximation and using Reiter's wave function we have found various spin correlation functions. We show that the different sign of hopping elements between the hole- and electron-doped system of high- T_c cuprates is responsible for the sharp difference of the polaron structure between the two systems with antiferromagnetism stabilized in the electron-doped case by carriers moving mainly on one sublattice.

PACS. 71.10.Fd Lattice fermion models (Hubbard model, etc.) – 71.27.+a Strongly correlated electron systems; heavy fermions

1 Introduction

Since the discovery of the high- T_c superconductors [1] there has been intense theoretical and experimental effort to find an accurate description of the properties of charge carriers in CuO_2 planes of high-temperature superconducting oxides (HTSO). The simplest approximation to the low-energy electronic states of strongly correlated systems is produced by the t - J model. Here, the antiferromagnetic (AF) correlations lead to the spectral functions with a single quasiparticle (QP) peak with low dispersion and a broad incoherent background at higher energies [2,3]. The extended t - t' - J [4,5] and t - t' - t'' - J [6] models, with the effective parameters t' and t'' derived from the multi-band tight-binding models [7], are able to reproduce the dispersion of low energy QP states in reasonable agreement with the photoemission measurements [8] of insulating $\text{Sr}_2\text{CuO}_2\text{Cl}_2$. The dynamics of holes was also studied in the simpler t - J^z model using numerical methods [9,10] and the pairing of holes was considered [3,11].

The main purpose of this work is to use Reiter's wave function [12] and calculate various correlation functions for different values of the superexchange interaction J . Here, we lean heavily on the work done in the context of the t - J and t - J^z models by Ramšak and Horsch (see Refs. [10,13]). We study the spin polaron in the slave fermion approach using a self-consistent Born approximation (SCBA) to evaluate the Green function [14,15]. This approach was successful in reproducing the results of exact diagonalization [16]. Although in the limit $J \rightarrow 0$ many magnon terms have to be included and the Green function is momentum dependent, it is possible to evaluate some correlation functions with the summation of noncrossing diagrams to any order.

Calculations of the deformation of the spin systems for one [17] and two holes [18] in the two-dimensional (2D) quantum AF state were performed by exact diagonalization of small clusters. In the t - J model the correlation functions describing the spatial structure of the spin polaron are power-law like leading to renormalization problems [19,10]. Here, the absence of spin fluctuations simplifies the analytical treatment of carrier motion in an AF background while the polaron shows an isotropic Gaussian decay.

The paper is organized as follows. In Section 2 we derive different correlation functions for the t - t' - t'' - J^z model. The numerical results obtained using Reiter's wave function are presented and analyzed in Section 3. In Section 4 we summarize the results and give general conclusions.

2 Model Hamiltonian

The extended Hubbard model with large on-site repulsion U compared with the hopping elements t , t' , t'' can be transformed to the following t - t' - t'' - J model [6],

$$\begin{aligned}
 H = & -t \sum_{\langle ij \rangle, \sigma} (\tilde{c}_{i\sigma}^\dagger \tilde{c}_{j\sigma} + \text{H.c.}) - t' \sum_{\langle\langle ij \rangle\rangle, \sigma} (\tilde{c}_{i\sigma}^\dagger \tilde{c}_{j\sigma} + \text{H.c.}) \\
 & - t'' \sum_{\langle\langle\langle ij \rangle\rangle\rangle, \sigma} (\tilde{c}_{i\sigma}^\dagger \tilde{c}_{j\sigma} + \text{H.c.}) \\
 & - \frac{t^2}{U} \sum_{i\sigma} \sum_{j' \neq j} (\tilde{c}_{j'\sigma}^\dagger n_{i-\sigma} \tilde{c}_{j\sigma} - \tilde{c}_{j'\sigma}^\dagger \tilde{c}_{i-\sigma}^\dagger \tilde{c}_{i\sigma} \tilde{c}_{j-\sigma}) \\
 & + J \sum_{\langle ij \rangle} \left[S_i^z S_j^z + \frac{\alpha}{2} (S_i^+ S_j^- + S_i^- S_j^+) \right], \quad (1)
 \end{aligned}$$

where $\tilde{c}_{i\sigma} = c_{i\sigma}(1 - n_{i-\sigma})$ while $\langle ij \rangle$, $\langle\langle ij \rangle\rangle$, and $\langle\langle\langle ij \rangle\rangle\rangle$ represent the nearest-, second- and third-neighbors,

^a e-mail: ufbala@jetta.if.uj.edu.pl

respectively. The superexchange interactions are characterized by the exchange coupling $J = 4t^2/U$ and the Ising limit is given by $\alpha = 0$. Here only the leading three-site terms have been included [16] which are omitted in the standard version of the t - J Hamiltonians [2].

Considering the motion of a single hole one has to implement the constraint of no double occupancy. Here we introduce the “slave fermion” representation for fermion operators [20], $c_{i\sigma}^\dagger = h_i b_{i\sigma}^\dagger$, with $b_{i\sigma}$ standing for a Schwinger boson at site i , subject to the constraint that $h_i^\dagger h_i + \sum_\sigma b_{i\sigma}^\dagger b_{i\sigma} = 1$ at each site. This automatically fulfills the condition of no double occupancy. Following the standard procedure [2, 14], considering mean-field theory in the Schwinger bosons and neglecting an irrelevant constant one finds the following Hamiltonian in the Ising limit,

$$H_z = \sum_{\mathbf{k}} \varepsilon(\mathbf{k}) h_{\mathbf{k}}^\dagger h_{\mathbf{k}} + \sum_{\mathbf{q}} \omega_0 a_{\mathbf{q}}^\dagger a_{\mathbf{q}} + \sum_{\mathbf{k}\mathbf{q}} \left[M_{\mathbf{k}-\mathbf{q}} h_{\mathbf{k}}^\dagger h_{\mathbf{k}-\mathbf{q}} a_{\mathbf{q}} + \text{H.c.} \right], \quad (2)$$

where $\omega_0 = 2J^z$ and $M_{\mathbf{k}} = \frac{zt}{\sqrt{N}} \gamma_{\mathbf{k}}$ with $\gamma_{\mathbf{k}} = \frac{1}{2}(\cos k_x + \cos k_y)$ and $z = 4$ in a 2D case. Here, $a_{\mathbf{q}}$ is Fourier transformation of Schwinger bosons,

$$a_{\mathbf{q}} = \sum_{i \in A} b_{i\downarrow} e^{i\mathbf{q}\cdot\mathbf{R}_i} + \sum_{j \in B} b_{j\uparrow} e^{i\mathbf{q}\cdot\mathbf{R}_j}, \quad (3)$$

where A and B are the sublattices of \uparrow - and \downarrow -spins in the Néel state, respectively.

Moreover, the free band $\varepsilon(\mathbf{k})$ for spinless $h_{\mathbf{k}}$ fermions is given by [5],

$$\varepsilon(\mathbf{k}) = zt'\eta_{\mathbf{k}} + zt''\gamma_{2\mathbf{k}} + \frac{zt^2}{U} (z\gamma_{\mathbf{k}}^2 - 1), \quad (4)$$

with $\eta_{\mathbf{k}} = \cos k_x \cos k_y$. In the presence of the three-site terms $\sim t^2/U$ the width of the free dispersion diverges $W_{\varepsilon(\mathbf{k})} \rightarrow \infty$ in the limit $J/|t| \rightarrow \infty$.

The Green function,

$$G(\mathbf{k}, \omega) = \frac{1}{\omega - \varepsilon(\mathbf{k}) - \Sigma(\mathbf{k}, \omega)}, \quad (5)$$

with the self-energy $\Sigma(\mathbf{k}, \omega)$ is calculated within the self-consistent Born approximation,

$$\Sigma(\mathbf{k}, \omega) = \sum_{\mathbf{q}} M_{\mathbf{k}-\mathbf{q}}^2 G(\mathbf{k}-\mathbf{q}, \omega - \omega_0). \quad (6)$$

In Figure 1 we present the free hole bands for the t - J model with three-site $\sim t^2/U$ terms and for the extended t - J model for the realistic parameters for hole- and electron-doped systems. As one can see, in the $(0, 0)$ - (π, π) direction $\varepsilon(\mathbf{k})$ has a minimum at $\mathbf{k} = (\pi/2, \pi/2)$ for all three parameter sets. At the $(\pi, 0)$ point further hoppings lead to a minimum (maximum) of the free dispersion in the electron (hole) doped case, respectively. As a result, the dispersion relation $\varepsilon(\mathbf{k})$ has the lowest value at

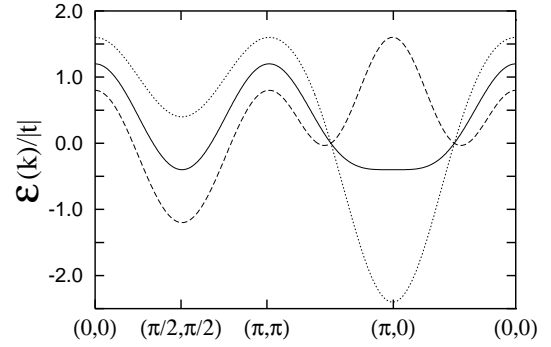


Fig. 1. Free hole bands calculated for $J^z/|t| = 0.4$ for the t - J^z model with the three-site terms (solid line) and the t - t' - t'' - J^z model with $t' = -0.3t$, $t'' = 0.2t$ and $t = 1$ (dashed line), $t = -1$ (dotted line).

the $(\pi/2, \pi/2)$ point both for the t - J model with $\sim t^2/U$ terms and for the extended model for one added hole. On the other hand, for parameters representing electron doping one finds the lowest value of $\varepsilon(\mathbf{k})$ for $\mathbf{k} = (\pi, 0)$. Thus, for the electron (hole) doped CuO_2 the single-carrier ground state corresponds to quasiparticles with momentum $\mathbf{k} = (\pi, 0)$ ($\mathbf{k} = (\pi/2, \pi/2)$), respectively.

Unlike in the t - J^z model here we have *momentum dependent* Green function leading to a more complex form of various correlation functions. Calculating the Green function, one can obtain the Reiter’s wave function [12, 13] of the following form,

$$|\Psi_{\mathbf{k}}^n\rangle = Z_{\mathbf{k}} \left[h_{\mathbf{k}}^\dagger + \sum_{\mathbf{q}_1} M_{\mathbf{k}_1} G(\mathbf{k}_1, \omega_1) h_{\mathbf{k}_1}^\dagger a_{\mathbf{q}_1}^\dagger + \dots + \sum_{\mathbf{q}_1 \dots \mathbf{q}_n} M_{\mathbf{k}_1} G(\mathbf{k}_1, \omega_1) \dots M_{\mathbf{k}_n} \times G(\mathbf{k}_n, \omega_n) h_{\mathbf{k}_n}^\dagger a_{\mathbf{q}_1}^\dagger \dots a_{\mathbf{q}_n}^\dagger \right] |0\rangle, \quad (7)$$

with the momentum $\mathbf{k}_n = \mathbf{k} - \mathbf{q}_1 - \dots - \mathbf{q}_n$ and energy $\omega_n = E_{\mathbf{k}} - n\omega_0$. The QP energy is determined by $E_{\mathbf{k}} = \varepsilon(\mathbf{k}) + \Sigma(\mathbf{k}, E_{\mathbf{k}})$, while $|\Psi_{\mathbf{k}}^n\rangle$ is normalized to 1 for,

$$Z_{\mathbf{k}} = \frac{1}{1 - \frac{\partial}{\partial \omega} \Sigma(\mathbf{k}, \omega)|_{\omega=E_{\mathbf{k}}}}. \quad (8)$$

When noncrossing diagrams are included the wave function $|\Psi_{\mathbf{k}}^n\rangle$ is exact. In a two-sublattice antiferromagnet with not very small J/t the QP moves mainly on one sublattice. Thus, we consider the linear combinations,

$$|\Psi_{\mathbf{k}\pm}^n\rangle = 2^{-1/2} [|\Psi_{\mathbf{k}}^n\rangle \pm |\Psi_{\mathbf{k}+\mathbf{Q}}^n\rangle], \quad (9)$$

where $\mathbf{Q} = (\pi, \pi)$ is the AF wave vector. As we evaluate the correlation functions for a hole at the bottom of the QP band only the real part of $G(\mathbf{k}, \omega_n)$ is nonzero.

3 Numerical results

The numerical calculations were performed for a 32×32 momentum-space mesh with energy resolution

$\delta\omega \sim 10^{-3}|t|$. In the wave function (9) the terms up to $n = 50$ were included for very small values of $J^z/|t|$. We adopted the nearest-neighbor hopping $|t| = 1$ as the energy unit. The sign of hopping elements changes between the hole and electron doping [21]. Here, we assume $t' = -0.3t$, $t'' = 0.2t$ with $t = 1$ (-1) corresponding to the hole (electron) doping, respectively [22]. The above hoppings with $t = 0.35$ eV can reproduce measured dispersion relation in $\text{Sr}_2\text{CuO}_2\text{Cl}_2$ [4, 8] and are consistent with the band structure of $\text{Bi}_2\text{Sr}_2\text{CaCuO}_2\text{O}_{8+\delta}$ and $\text{YBa}_2\text{Cu}_3\text{O}_{7-\delta}$ compounds [23]. Similar parameters with $t = -0.35$ eV were used by Kim *et al.* [22] to describe quasiparticle spectra in electron doped $\text{Nd}_{1.85}\text{Ce}_{0.15}\text{CuO}_4$ [24].

Knowing the wave function we can calculate various correlation functions describing the deformation of the AF order around a hole. First, we have to calculate the norm $\mathcal{N}_{\mathbf{k}}^{(n)}$ to estimate where the wave function can be truncated,

$$\mathcal{N}_{\mathbf{k}}^{(n)} = \langle \Psi_{\mathbf{k},\pm}^{(n)} | \Psi_{\mathbf{k},\pm}^{(n)} \rangle = \sum_{m=1}^n A_{\mathbf{k}}^{(m)}, \quad (10)$$

where the distribution functions,

$$A_{\mathbf{k}}^{(m)} = Z_{\mathbf{k}} \prod_{j=1}^m \sum_{\mathbf{q}} M_{\mathbf{q}}^2 G^2(\mathbf{q}, \omega_j), \quad (11)$$

for $m > 0$ and $A_{\mathbf{k}}^{(0)} = Z_{\mathbf{k}}$.

In order to estimate the number of magnon terms needed in the wave function we calculated the distribution functions $A_{\mathbf{k}}^{(n)}$ corresponding to a noncrossing diagram with n magnons excited. The $A_{\mathbf{k}}^{(n)}$ coefficients are presented in Figure 2 for the extended t - J^z model with realistic parameters for hole- and electron-doped HTSOs. In the regime of strong coupling ($J^z/|t| \ll 1$) and for parameters representing hole doped materials $A_{\mathbf{k}}^{(n)}$ has a maximum at a finite value n which increases with decreasing $J^z/|t|$ (see Fig. 2a). Similar behavior was found in the t - J^z model (see Fig. 4 of Ref. [10]). Quite different dependence of $A_{\mathbf{k}}^{(n)}$ with n is found for electron doping (Fig. 2b) where one finds its monotonous decrease with increasing n for $J^z/|t|$ even as small as 0.002.

The total number of magnons building up our spin polaron in the Ising limit can be easily calculated as,

$$\langle n \rangle = \langle \Psi_{\mathbf{k},\pm}^{(n)} | \sum_{\mathbf{q}} a_{\mathbf{q}}^\dagger a_{\mathbf{q}} | \Psi_{\mathbf{k},\pm}^{(n)} \rangle = \sum_{m=1}^n m A_{\mathbf{k}}^{(m)}. \quad (12)$$

The dependence of $\langle n \rangle$ with $J/|t|$ is presented in Figure 3. Both in the t - J model and for parameters representing hole doping we have recovered the results by Ramšak and Horsch [10] with $\langle n \rangle \approx 1.4(|t|/J^z)^{1/3}$ consistent with the string potential of overturned spins created by the carrier motion. For large $J^z/|t| > 2$ the asymptotic behavior $\langle n \rangle \sim (|t|/J^z)^2$ is reached. Quite different dependence of $\langle n \rangle$ is found for parameters representing electron doping where in the $J^z/|t| \rightarrow 0$ limit much less magnons are excited with no simple scaling for $J^z/|t|$ down to 0.002.

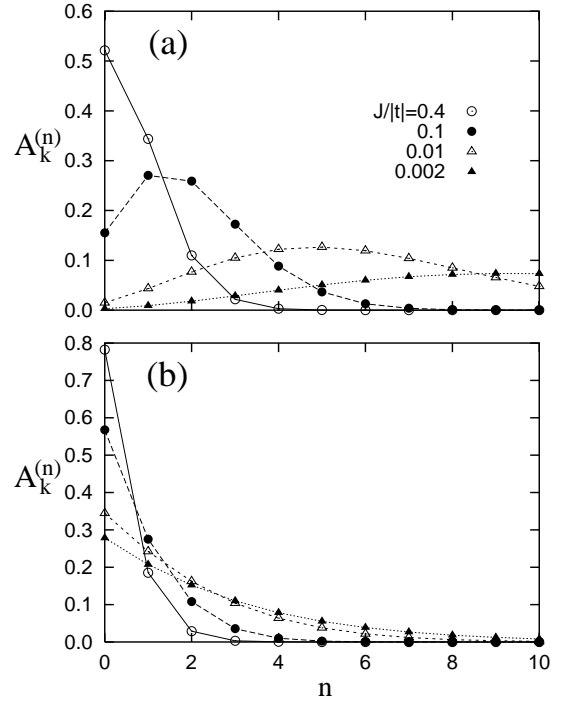


Fig. 2. The distribution of the number of magnons $A_{\mathbf{k}}^{(n)}$ as a function of n for various $J^z/|t|$ calculated for $t' = -0.3t$, $t'' = 0.2t$ and (a) $t = 1$, (b) $t = -1$.

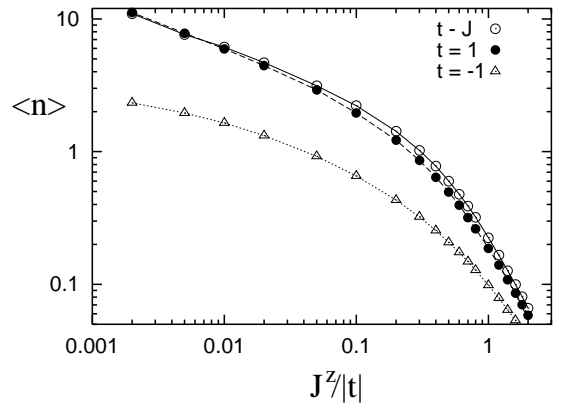


Fig. 3. Average number of magnons $\langle n \rangle$ as a function of $J^z/|t|$ calculated for the t - J^z model (solid line) and the t - t' - t'' - J^z model with $t' = -0.3t$, $t'' = 0.2t$ and $t = 1$ (dashed line), $t = -1$ (dotted line).

The distribution of magnons around a hole can be defined by $N_{\mathbf{R}} = \langle h_0^\dagger h_0 a_{\mathbf{R}}^\dagger a_{\mathbf{R}} \rangle$ where the Fourier transform, $a_{\mathbf{R}}^\dagger = \sum_{\mathbf{q}} e^{-i\mathbf{q}\mathbf{R}} a_{\mathbf{q}}^\dagger$, and the average is calculated with respect to the wave function (9), $\langle \dots \rangle = \langle \Psi_{\mathbf{k}\pm}^n | \dots | \Psi_{\mathbf{k}\pm}^n \rangle$. The explicit form of $N_{\mathbf{R}}$ is presented in Appendix A. Now, the size of a polaron can be characterized by the average radius,

$$R_{\text{av}} = \langle n \rangle^{-1} \sum_{\mathbf{R}} |\mathbf{R}| N_{\mathbf{R}} \quad (13)$$

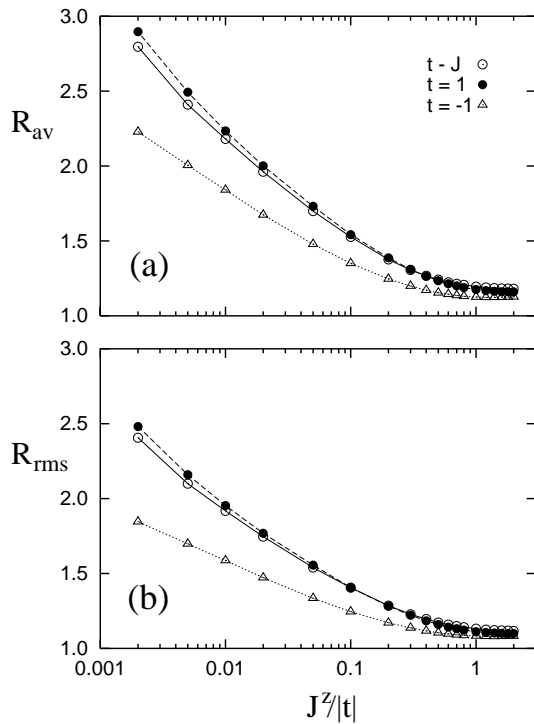


Fig. 4. The average radius (a) and the root-mean-square radius (b) as a function of $J^z/|t|$ calculated for the t - J^z model (solid lines) and the t - t' - t'' - J^z model with $t' = -0.3t$, $t'' = 0.2t$ and $t = 1$ (dashed lines), $t = -1$ (dotted lines).

and the root-mean-square radius,

$$R_{\text{rms}} = \left(\langle n \rangle^{-1} \sum_{\mathbf{R}} |\mathbf{R}|^2 N_{\mathbf{R}} \right)^{1/2} \quad (14)$$

R_{av} and R_{rms} as functions of $J^z/|t|$ are shown in Figure 4. For the t - J^z model and the hole-doped case of the extended model the root-mean-square radius of the polaron for $J^z < 0.1t$ can be fitted with $R_{\text{rms}} = 1.07(t/J)^{0.154}$ and $1.07(t/J)^{0.161}$, respectively. The radius calculated for the t - J^z model is slightly different than one evaluated by Ramšak *et al.* in reference [10]. This difference is made by the t^2/U three-site terms which are small for $J^z/t < 0.1$. In the case of the electron doped t - t' - t'' - J^z model for $0.002 < J^z/|t| < 0.1$ we found the size of the polaron increasing logarithmically with decreasing $J^z/|t|$ and fitted with $R_{\text{rms}} = 0.226 \ln(|t|/J) + 0.81$ for $J^z/|t| < 0.1$.

Another correlation function describing the spatial distribution of spin around the hole is the average of the z component of spin, $S_{\mathbf{R}} = \langle h_0^\dagger h_0 S_{\mathbf{R}}^z \rangle$, with $S_{\mathbf{R}}^z = e^{i\mathbf{Q}\mathbf{R}} (\frac{1}{2} - a_{\mathbf{R}}^\dagger a_{\mathbf{R}})$. The explicit form of $S_{\mathbf{R}}$ is given in Appendix A. We have found a striking difference in the distribution of spins when calculated for hole- and electron-doped systems. For our model with parameters representing hole doping one can see a well visible polaron around a hole with a negligible background contribution $S_0^z \approx 0.001$ (see Fig. 5a), where $S_0^z = \lim_{|\mathbf{R}| \rightarrow \infty} |S_{\mathbf{R}}^z|$. A very similar polaron was found by Ramšak and Horsch in the t - J^z model (compare Fig. 5a with Fig. 9a of Ref. [10]). In

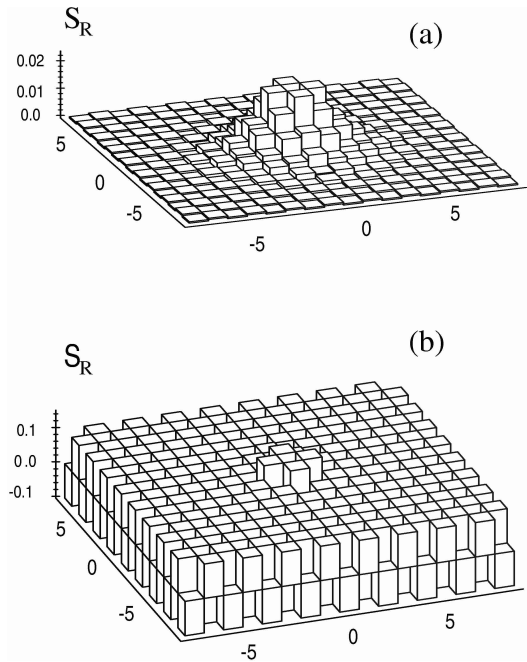


Fig. 5. Distribution of the z component of the spin $S_{\mathbf{R}}^z$ around the moving hole for $J^z/|t| = 0.01$ found for the t - t' - t'' - J^z model with $t' = -0.3t$, $t'' = 0.2t$ and $t = 1$ (a), $t = -1$ (b).

contrast, when parameters representing electron doping are assumed one can find the $S_{\mathbf{R}}$ function dominated by large background $S_0^z \approx 0.1$ (see Fig. 5b). As pointed out by Ramšak and Horsch [10], $2S_0^z$ represents the difference in the probability of the hole sitting on sublattice A or B. Thus, even for $J^z/|t|$ as small as 0.01 this difference of visiting the two sublattices by an electron is about 20% in the electron-doped case.

Finally, we check the conservation of the z component of the total spin $S_{\text{tot}}^z = \sum_{\mathbf{R} \neq 0} S_{\mathbf{R}}^z$ which consists of two parts (see Eq. (20)). S_{tot}^z deviates from 0.5 by no more than 10% in the whole range of $J^z/|t|$ with the minimum value in the intermediate-coupling regime $J^z \approx 0.1|t|$ for the t - J^z and the hole-doped t - t' - t'' - J^z models whereas in the electron doped case the minimum of S_{tot}^z is found for $J^z \approx 0.01|t|$ (see Fig. 6). The S_0^z part of the spin-correlation function $S_{\mathbf{R}}$ (giving nonvanishing background in Fig. 5) is presented in Figure 6b. In all three cases S_0^z decreases with decreasing spin stiffness and $S_0^z \rightarrow 0$ for $J^z/|t| \rightarrow 0$. For realistic $J^z/|t| = 0.4$ the difference in the probability of a carrier being on one or the other sublattice is about 17%, 27%, and 62% for the t - J^z model, t - t' - t'' - J^z model with hole- and electron doping, respectively. For the t - J^z model the three-site terms enhance the tendency towards one sublattice motion of a hole (compare solid line in Fig. 6b with Fig. 11 of Ref. [10]). The results for the electron-doped system indicates that an added electron can stabilize the AF long range order by moving mainly over one sublattice. This is not the case when an electron is removed from the half filled system.

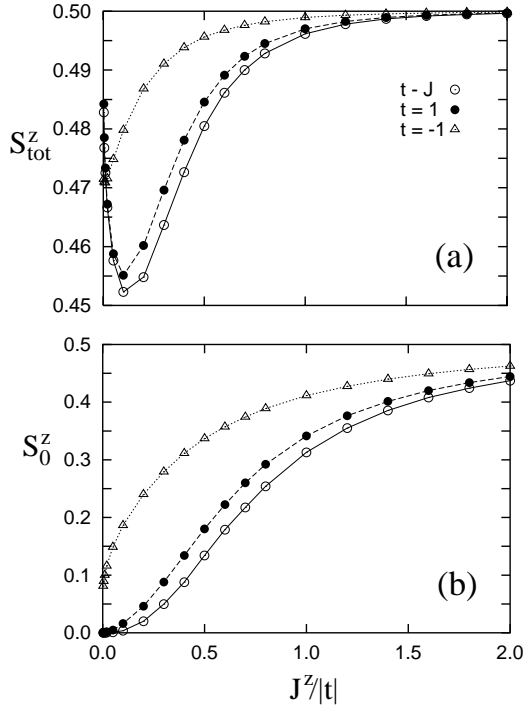


Fig. 6. The total spin S_{tot}^z (a) and its component S_0^z (b) as a function of $J^z/|t|$ calculated for the t - J^z model (solid lines) and the t - t' - t'' - J^z model with $t' = -0.3t$, $t'' = 0.2t$ and $t = 1$ (dashed lines), $t = -1$ (dotted lines).

4 Conclusions

We have presented a systematic way to calculate various spin correlation functions in the t - t' - t'' - J^z model. Emphasis was put on the strong-coupling limit, $J^z/|t| \ll 1$, where the Reiter's wave function is dominated by higher order terms. As the magnon mode is dispersionless (but not the Green function itself) it is possible to express correlation function elements analytically and perform the summation of respective diagrams to any order. Of key importance to our approach is the vertex function $M_{\mathbf{k}-\mathbf{q}}$ (see Eq. (2)) depending only on $\mathbf{k} - \mathbf{q}$ momentum.

As presented in the previous section the spin polarons found for the electron-doped case are qualitatively different from those found for the hole-doped case or for the t - J model [21]. For small $J^z/|t|$ an added electron moves mainly on one sublattice avoiding the disturbance of the AF order while a hole propagates mainly by the exchange of collective excitations. For realistic values of $J^z/|t| \approx 0.4$ for HTSOs the average number of magnons excited in the ground state is about one when a hole is added to the Néel state and no more than 0.2 in the electron-doped case.

The main limitation of this approach is the absence of spin fluctuations. A hole (electron) hops in a Néel state creating a "string" of overturned spins which are not allowed to flip spontaneously. The validity of ignoring the propagation of spin excitations is justified by the fact that in the limit $J^z \ll |t|$ a linear potential left by turned over spins [15] is weak making the propagation of a hole (electron) not much restricted. However, for larger J^z the

mobility of a carrier is strongly restricted to one sublattice. Moreover, in the t - J model one can find a well defined quasiparticles but the size of a polaron characterized by R_{av} and R_{rms} is diverging [10] while the wave function can be evaluated numerically only to a few magnon terms which is hardly enough in the limit $J \ll |t|$.

I thank A. M. Oleś and P. Horsch for useful discussions and acknowledge the financial support by the Committee of Scientific Research (KBN) of Poland, Project No. 2 P03B 175 14.

Appendix A: The spatial distribution functions

Below we present the analytical expressions of correlation functions $N_{\mathbf{R}}$ and $S_{\mathbf{R}}$ evaluated in this paper. In the Ising limit the distribution of magnons around a hole has the following form,

$$N_{\mathbf{R}} = \frac{1}{N} \sum_{\mathbf{q}_1, \mathbf{q}_2} e^{i(\mathbf{q}_1 - \mathbf{q}_2)\mathbf{R}} \times \sum_{p=1}^n \left[\sum_{m=1}^{p-1} W^{(p,m)}(\mathbf{q}_1, \mathbf{q}_2) + W^{(p)}(\mathbf{q}_1, \mathbf{q}_2) \right], \quad (15)$$

with,

$$W^{(p,m)}(\mathbf{q}_1, \mathbf{q}_2) = A_{\mathbf{k}}^{(m-1)} T_{2\mathbf{k}}^{(m)}(\mathbf{q}_1, \mathbf{q}_2) \times \prod_{j=m+2}^p T_{1\mathbf{k}}^{(j)}(\mathbf{q}_1, \mathbf{q}_2), \quad (16)$$

for $0 < m < p$ and,

$$W^{(p)}(\mathbf{q}_1, \mathbf{q}_2) = Z_{\mathbf{k}} M_{\mathbf{k}-\mathbf{q}_1} M_{\mathbf{k}-\mathbf{q}_2} G(\mathbf{k} - \mathbf{q}_1, \omega_1) \times G(\mathbf{k} - \mathbf{q}_2, \omega_1) \prod_{j=2}^p T_{1\mathbf{k}}^{(j)}(\mathbf{q}_1, \mathbf{q}_2). \quad (17)$$

The functions $T_{1(2)\mathbf{k}}^{(j)}(\mathbf{q}_1, \mathbf{q}_2)$ depend on the Green function $G(\mathbf{q}, \omega)$ and the hole-magnon vertex $M_{\mathbf{q}}$ as follows,

$$T_{1\mathbf{k}}^{(j)}(\mathbf{q}_1, \mathbf{q}_2) = \sum_{\mathbf{q}} M_{\mathbf{q}-\mathbf{q}_1} M_{\mathbf{q}-\mathbf{q}_2} G(\mathbf{q} - \mathbf{q}_1, \omega_j) \times G(\mathbf{q} - \mathbf{q}_2, \omega_j), \quad (18)$$

and,

$$T_{2\mathbf{k}}^{(j)}(\mathbf{q}_1, \mathbf{q}_2) = \sum_{\mathbf{q}} M_{\mathbf{q}}^2 M_{\mathbf{q}-\mathbf{q}_1} M_{\mathbf{q}-\mathbf{q}_2} G^2(\mathbf{q}, \omega_j) \times G(\mathbf{q} - \mathbf{q}_1, \omega_{j+1}) G(\mathbf{q} - \mathbf{q}_2, \omega_{j+1}). \quad (19)$$

In a similar way one can evaluate the distribution of the z component of the spin at a distance \mathbf{R} from a hole,

$$S_{\mathbf{R}} = \pm e^{i\mathbf{q}\mathbf{R}} \left[S_0^z - \frac{1}{N} \sum_{\mathbf{q}_1, \mathbf{q}_2} e^{i(\mathbf{q}_1 - \mathbf{q}_2)\mathbf{R}} \sum_{p=1}^n (-1)^p \times \left(\sum_{m=1}^{p-1} W^{(p,m)}(\mathbf{q}_1, \mathbf{q}_2) + W^{(p)}(\mathbf{q}_1, \mathbf{q}_2) \right) \right], \quad (20)$$

with,

$$S_0^z = \frac{1}{2} \sum_{j=0}^n (-1)^j A_{\mathbf{k}}^{(j)}. \quad (21)$$

The details of the construction rule for the diagrams included in $N_{\mathbf{R}}$ and $S_{\mathbf{R}}$ can be found in the recent paper by Ramšak and Horsch (see Ref. [10]).

References

1. J.G. Bednorz, K.A. Müller, Z. Phys. B **64**, 189 (1986).
2. G. Martínez, P. Horsch, Phys. Rev. B **44**, 317 (1991).
3. E. Dagotto, Rev. Mod. Phys. **66**, 763 (1994).
4. A. Nazarenko, K.J.E. Vos, S. Haas, E. Dagotto, R.J. Gooding, Phys. Rev. B **51**, 8676 (1995); T. Xiang, J.M. Wheatley, *ibid.* **54**, 12 653 (1996); R. Eder, Y. Ohta, G.A. Sawatzky, *ibid.* **55**, 3414 (1997); F. Lema, A.A. Aligia, *ibid.* **55**, 14 092 (1997); Y. Shibata, T. Tohyama, S. Maekawa, *ibid.* **59**, 1840 (1999).
5. J. Bala, A.M. Oleś, J. Zaanen, Phys. Rev. B **52**, 4597 (1995).
6. B. Kyung, R.A. Ferrell, Phys. Rev. B **54**, 10 125 (1996); V.I. Belinicher, A.L. Chernyshev, V.A. Shubin, *ibid.* **54**, 14 914 (1996).
7. J.H. Jefferson, H. Eskes, L.F. Feiner, Phys. Rev. B **45**, 7959 (1992); L.F. Feiner, J.H. Jefferson, R. Raimondi, *ibid.* **53**, 8751 (1996); O.K. Andersen, A.I. Liechtenstein, O. Jepsen, F. Paulsen, J. Phys. Chem. Solids **56**, 1573 (1995).
8. B.O. Wells, Z.X. Shen, A. Matsuura, D.M. King, M.A. Kastner, M. Greven, R.J. Birgeneau, Phys. Rev. Lett. **74**, 964 (1995); J.J.M. Pothuizen, R. Eder, N.T. Hien, M. Matoba, A.A. Menovsky, G.A. Sawatzky, *ibid.* **78**, 717 (1997).
9. T. Barnes, E. Dagotto, A. Moreo, E.S. Swanson, Phys. Rev. B **40**, 10 977 (1989); J.A. Riera, E.P. Dagotto, *ibid.* **47**, 15 346 (1993).
10. A. Ramšak, P. Horsch, Phys. Rev. B **57**, 4308 (1998).
11. S. Trugman, Phys. Rev. B **37**, 1597 (1988); B. Shraiman, E. Siggia, Phys. Rev. Lett. **60**, 740 (1988); A.L. Chernyshev, P.W. Leung, Phys. Rev. B **60**, 1592 (1999).
12. G.F. Reiter, Phys. Rev. B **49**, 1536 (1994).
13. A. Ramšak, P. Horsch, Phys. Rev. B **48**, 10 559 (1993).
14. S. Schmitt-Rink, C.M. Varma, A.E. Ruckenstein, Phys. Rev. Lett. **60**, 2793 (1989).
15. C.L. Kane, P.A. Lee, N. Read, Phys. Rev. B **39**, 6880 (1989).
16. K.J. von Szczepanski, P. Horsch, W. Stephan, M. Ziegler, Phys. Rev. B **41**, 2017 (1990).
17. V. Elser, D.A. Huse, B.I. Shraiman, E.D. Siggia, Phys. Rev. B **41**, 6715 (1990); J. Inoue, S. Maekawa, J. Phys. Soc. Jpn **59**, 3467 (1990).
18. J. Bonča, P. Prelovšek, I. Sega, Phys. Rev. B **39**, 7074 (1989).
19. P.W. Anderson, Phys. Rev. Lett. **64**, 1839 (1990).
20. S.E. Barnes, J. Phys. F **6**, 1375 (1976); *ibid.* **7**, 2637 (1977); P. Coleman, Phys. Rev. B **29**, 3035 (1984).
21. T. Tohyama, S. Maekawa, Phys. Rev. B **49**, 3596 (1994); R.J. Gooding, K.J.E. Vos, P.W. Leung, *ibid.* **50**, 12 866 (1994).
22. C. Kim, P.J. White, Z.-X. Shen, T. Tohyama, Y. Shibata, S. Maekawa, B.O. Wells, Y.J. Kim, R.J. Birgeneau, M.A. Kastner, Phys. Rev. Lett. **80**, 4245 (1998).
23. O.K. Andersen, O. Jepsen, A.I. Liechtenstein, I.I. Mazin, Phys. Rev. B **49**, 4145 (1994).
24. D.M. King, Z.-X. Shen, D.S. Dessau, B.O. Wells, W.E. Spicer, A.J. Arko, D.S. Marshall, J. DiCarlo, A.G. Loeser, C.H. Park, E.R. Ratner, J.L. Peng, Z.Y. Li, R.L. Greene, Phys. Rev. Lett. **70**, 3159 (1993); R.O. Anderson, R. Claessen, J.W. Allen, C.G. Olson, C. Janowitz, L.Z. Liu, J.-H. Park, M.B. Maple, Y. Dalichaouch, M.C. de Andrade, R.F. Jardim, E.A. Early, S.-J. Oh, W.P. Ellis, *ibid.* **70**, 3163 (1993).